

An effective tunneling description of voltage switching in Josephson Junctions driven by time varying fields

Christian Kraglund Andersen* and Klaus Mølmer

Department of Physics and Astronomy, Aarhus University, DK-8000 Aarhus, Denmark

(Dated: November 9, 2021)

We propose to use a time dependent imaginary potential to describe quantum mechanical tunnelling through time dependent potential barriers. We use Gamow solutions for the stationary tunneling problem to justify our choice of potential, and we apply our ansatz to describe voltage switching in a driven current-biased Josephson Junction. The Josephson Junction phase variable experiences a tilted washboard potential with metastable trapped states, and our description reproduces a number of features associated with the switching dynamics of the phase variable from trapped to running states, in particular the dependence on bias current and parameters of a driving field. Our calculations also explore the potential of the fixed current-biased Josephson Junction as a field amplitude detector.

PACS numbers: 85.30.Mn, 85.25.Cp, 03.65.Ta, 03.65.Xp

I. INTRODUCTION

Circuit quantum electrodynamics has reached an experimental state of perfection that makes man-made devices compete with, or supersede, natural, microscopic quantum systems in terms of their quantum interaction and control properties, while at the same time retaining their fundamental interest as macroscopic quantum systems^{1,2}. Among the most interesting devices are the Current-Biased Josephson Junction (CBJJ) as their quantum level structure permits identification and control of pairs of states, which may be used as qubits for the realization of quantum information processing³. Recently, the CBJJ has also been suggested as a sensitive microwave photodetector^{4,5}. The phase variable associated with the superconductor is trapped in a washboard potential, see Fig.1, but it can be excited by the radiation field into states that undergo tunneling to running states observed as a voltage drop over the device. This switching can occur due to thermal activation⁶ and due to macroscopic quantum tunneling. In this treatment the contribution from thermal activation will be neglected.

A weak field-induced modulation of the trapping potential can be treated as a perturbation, coupling the ground trapped eigenstate resonantly to an excited state which is subject to tunneling, and good agreement with experimental results has been obtained⁷⁻¹⁰. In this paper we will describe the wave-function of the phase variable in a CBJJ subject to a strongly modified potential dynamically tilted by a microwave field. This case is not amenable to the weak field description, and instead, we shall formally describe the tunneling process by wave packet propagation in a time dependent imaginary potential (TDIP), such that the switching into the voltage state is treated as a dynamical loss process. In this way we both determine the time dependent probability for the switching to occur and we appropriately describe the evolution of the wave function conditioned on no switching event being detected.

Tunneling is a widely observed phenomenon in quantum mechanics, and for tunneling through stationary barriers

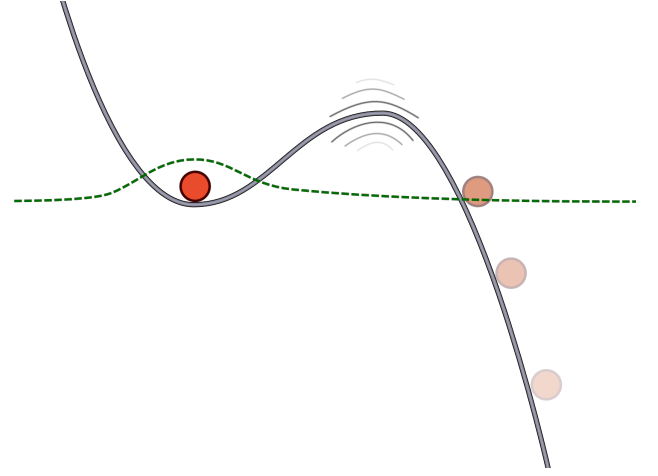


FIG. 1. (Color online) A of a particle trapped in a washboard potential. This is the potential experienced by the phase in a CBJJ. The dashed (green) line is a sketch of the ground state wavefunction. In this potential there is chance that the phase particle tunnels out of the potential. This chance is increased if the barrier is driven by a microwave field.

scattering theory and good approximations based on the JWKB method are available and easy to evaluate¹¹. For the general dynamical case such simple approximations do not apply. The part of the wave function that has not yet tunneled is evolving within the trapping region, and it encounters the tunnel barrier in a highly non-trivial manner. While the Schrödinger equation is well defined in a time dependent potential, the handling of the scattering continuum components of the wave function is impeded by the demand for precise calculations on a very large interval of the coordinate variable. In this paper we propose a new, effective ansatz to handle tunneling in a time dependent potential. The method addresses the general case of tunneling, but we will focus our attention on the current-biased Josephson junction, and we will use our method on several different cases, where the results can be compared with experiments.

The paper is organized as follows. In Sec. II, we introduce the CBJJ variables and dynamics. In Sec. III, we define the tunneling problem, we motivate our TDIP description, and we provide an explicit time dependent expression for the imaginary potential applied in our numerical studies. In Sec. IV, we use our method to study different regimes of switching dynamics with increasing bias currents applied to the CBJJ. In Sec. V we fix the bias current and we analyze the performance of the Josephson junction as a field detector by examination of the switching properties under application of a driving field. Sec. VI concludes the paper.

II. THE DYNAMICS OF A CBJJ

The Josephson Junction is composed of two superconductors, R(ight) and L(eft), separated by a thin isolating layer. The macroscopic wave functions of R and L, $\psi_{R,L}$ differ by a phase factor $\psi_L = e^{i\phi}\psi_R$, which constitutes the macroscopic quantum degree of freedom of the system. This phase can be described¹² as a quantum particle with mass $M = C(\Phi_0/2\pi)^2$, where C is the capacitance of the junction and $\Phi_0 = \frac{h}{2e}$ is the flux quantum. The particle experiences a potential

$$U_0(\phi) = -E_J(I\phi + \cos\phi) \quad (1)$$

where $E_J = \frac{I_c\Phi_0}{2\pi}$ is the Josephson energy and $I = \frac{I_b}{I_c}$, with I_b being the bias current applied to the junction. When I_b exceeds the critical current I_c , the potential tilt dominates the harmonic variation with ϕ , and the phase becomes classically unbound.

We further include the interaction of the CBJJ with a time dependent microwave field via the potential term,

$$U_{mw} = -E_J\eta\phi\sin(\omega_{mw}t) \quad (2)$$

where η is proportional to the field amplitude.

The CBJJ is thus described by the time-dependent Schrödinger equation

$$\begin{aligned} i\hbar\frac{\partial}{\partial t}\psi(\phi,t) &= H(t)\psi(\phi,t) \\ &= \left(-\frac{\hbar^2}{2M}\frac{\partial^2}{\partial\phi^2} + U(\phi,t)\right)\psi(\phi,t) \end{aligned} \quad (3)$$

with $U(\phi,t) = U_0 + U_{mw}$. This time dependent potential is sketched in Fig. 1, indicating also the tunneling process, responsible for the switching of the Josephson junction.

III. TUNNELING OF THE JOSEPHSON JUNCTION PHASE

A. Tunneling loss and complex absorbing potentials

The Josephson junction phase variable described by the Schrödinger equation (3) leaves the local potential

minimum by tunneling, and we shall obtain an effective, approximate theory for the tunneling dynamics. Following the early description by Gamow¹¹, one can describe tunneling by eigenfunctions of the time-independent Hamilton operator. If these functions are chosen with outgoing, radiating boundary conditions and used as a wave function basis, we effectively redefine the scalar product on the system Hilbert space, and the original Hamiltonian is not Hermitian. This in turn leads to the emergence of complex eigenvalues, and the loss of norm associated with the imaginary part of the energy eigenvalues represents the probability of tunnelling^{13–15}. Effective non-Hermitian Hamiltonians also emerge in the quantum optics and quantum measurement theory, where they govern the evolution of a quantum system conditioned on the absence of absorption or loss events. In these theories, the decreasing norm of the state vector also denotes the probability for the evolution to occur without these events happening, while one may simulate the complete dynamics by suitable application of "quantum jump" operators^{16–18}.

At a given time the tunneling probability is governed by the wave function obtained by propagating with our non-Hermitian Hamiltonian, *i.e.*, the state conditioned on the detection of no previous switching events. The amount of trapped phase population and its actual wave function therefore yields the local loss rate due to tunneling and the whole time dependent dynamics should be well described by the Gamow vectors and their complex eigenvalues. Another approach to yield complex eigenvalues is by directly implementing a non-Hermitian Hamiltonian with respect to the original Hilbert space of square integrable wave functions, for example by the introduction of a complex absorbing potential (CAP). A properly designed CAP may thus describe the same essential physics as the Gamow vectors, *i.e.*, the evolution of the unnormalized states may yield identical or very similar wave function behaviour in the spatial and temporal range of interest¹⁹.

There is a rich literature²⁰ on the identification of suitable CAPs, but since we shall be dealing with the further complexity of tunneling through a time dependent potential, we shall merely propose a simple, physically motivated *ansatz* for our time dependent imaginary potential (TDIP), $V_{im}(\phi,t)$, and solve the time-dependent Schrödinger equation

$$i\hbar\frac{\partial}{\partial t}\psi(\phi,t) = H(t)\psi(\phi,t) - iV_{im}(\phi,t)\psi(\phi,t). \quad (4)$$

B. Outgoing states and absorbing potential

An imaginary absorbing potential, extending beyond the outer turning point of a potential barrier would seem a natural candidate to remove the tail of the wave function as tunneling develops. Since we want the potential to remove the projection of our wave function on the running states in that region, it is useful to apply approximate

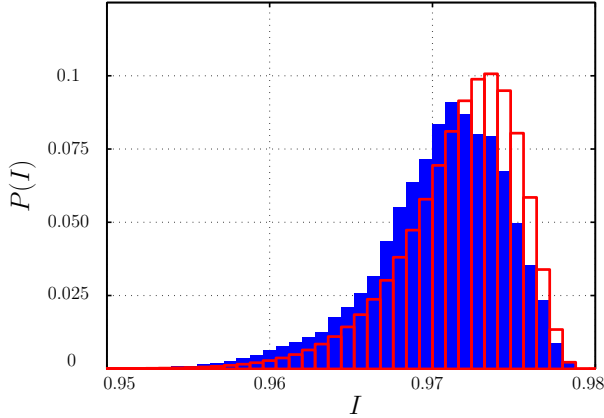


FIG. 2. (Color online) Blue (solid) bars is the switching current distribution simulated with an absorbing potential. Red (hollow) bars is calculated by Eq. (9). We have chosen C and R such that $\omega_0 = 0.0183 E_J/\hbar$ and $\zeta = 8.4 \times 10^{-4} E_J$. The bias current is increased linearly from $I = 0.2$ at a slow rate. $dI/dt = \frac{5E_J}{6\hbar}$. Results are shown for $I > 0.95$.

solutions for their position (phase) and time dependence in our ansatz for the TDIP. From²¹ we have an approximate expression for the running state of the Josephson junction phase variable $\phi > \phi_{turn}$, in the linear potential region beyond the outer classical turning point of the potential barrier ϕ_{turn} ,

$$\psi_{out}(\phi, t) = \sqrt{\frac{\Gamma}{\sqrt{2\phi'}\Phi_0\omega_p}} e^{i\frac{\hbar\omega_p\phi'^{3/2}}{6\sqrt{2}E_J} - \left(i\frac{\omega}{\omega_p} + \frac{\Gamma}{2\omega_p}\right)(t\omega_p - \sqrt{2\phi'})} \quad (5)$$

with $\phi' = \phi - \phi_0$, where ϕ_0 is the initial equilibrium position (bottom of the well) and $\hbar\omega$ is the energy difference between the bottom of the well and the energy of the lowest quasi-bound state. We have further introduced the frequency parameter $\omega_0 = \sqrt{\frac{2\pi I_c}{C\Phi_0}}$ and the plasma frequency $\omega_p = \omega_0(1 - I^2)^{1/4}$. The wavefunction (5) is defined for $t\omega_p > \sqrt{2\phi'}$, and we assume $I < 1$. The rate parameter Γ in (5) which attains a definite value in a static potential, will be briefly discussed below.

Our aim is to remove the projection of our time dependent wave function $|\psi(t)\rangle$ on a suitable set of running states of the form (5), $P_{out}|\psi\rangle = \sum_{\psi_{out}} |\psi_{out}\rangle \langle\psi_{out}|\psi\rangle$. We model this operation by a time-dependent complex potential, obtained as an integral over different running states, emitted within the past interval of time Δt ,

$$V_{im}(\phi, t) = \beta \int_{t-\Delta t}^t |\psi_{out}(\phi, t')|^2 dt'. \quad (6)$$

The parameter β serves both as an adjustable strength parameter and as a convenient normalization for the temporal integration. We assume a constant value of Γ and

Δt , with $\Delta t^{-1} \ll \Gamma \ll \omega_p$, and we evaluate the integral (6) only for values ϕ larger than the outer turning point, ϕ_{turn} , of the potential. The dependence on Γ drops out, and we obtain

$$V_{im}(\phi, t) = \begin{cases} \frac{\beta}{\sqrt{2\phi}\Phi_0\omega_p(t)} & \text{for } \phi > \phi_{turn}(t) \\ 0 & \text{for } \phi < \phi_{turn}(t). \end{cases} \quad (7)$$

Here, we recall the time-dependence of the plasma frequency as the effective bias-current is changing with time.

Unlike normal CAPs used in time-independent problems, this potential is modelled to absorb the running state components (5) pertaining to the time dependent Hamiltonian, and our ansatz imaginary potential indeed attains finite values only beyond the time dependent outer classical turning point of the real potential. We emphasize that (7) is only an ansatz, but it ensures that the depletion of the wave function norm is properly associated with the probability that the particle has tunnelled through the barrier.

While it is generally a challenge to design CAPs that do not reflect part of the wave packets impinging on them, our application only concerns the small wave function amplitude that has tunneled through the real potential barrier, and we have verified that reflection is insignificant in our calculations. To account for the running solution, the TDIP must furthermore suppress the wave function before it hits and gets reflected by the border of the grid used for the calculation, and a sufficiently large grid is readily identified in the numerical calculations.

C. Junction resistance and friction

We have now presented our candidate TDIP, but before we proceed to numerical examples let us include the junction resistance, R , which leads to friction for the phase variable ϕ . Methods have been developed to incorporate friction and Brownian motion in quantum mechanics,^{22,23} and assuming the zero-temperature and Markovian limit, a non-linear imaginary potential term, $-i\zeta(\phi - \langle\phi\rangle_t)^2$ may be added to the Hamiltonian, where $\zeta \propto \frac{1}{RC}$. This term decoheres the spatial wave function and penalizes large variations of ϕ around its mean. It also leads to a loss of norm, albeit on a typically slower scale than the tunneling dynamics. We shall include this term here, but we shall renormalize the wave function with respect to the loss it incurs, so that we unambiguously associate the wave function loss of norm with the tunneling dynamics.

To summarize, we treat the entire problem by solving the non-linear Schrödinger equation

$$i\hbar \frac{\partial}{\partial t} \psi(\phi, t) = \left(-\frac{\hbar^2}{2M} \frac{\partial^2}{\partial \phi^2} + U(\phi, t) \right) \psi(\phi, t) - iV_{im}(\phi, t) \psi(\phi, t) - i\zeta \left(\phi - \langle\phi\rangle_t \right)^2 \psi(\phi, t) \quad (8)$$

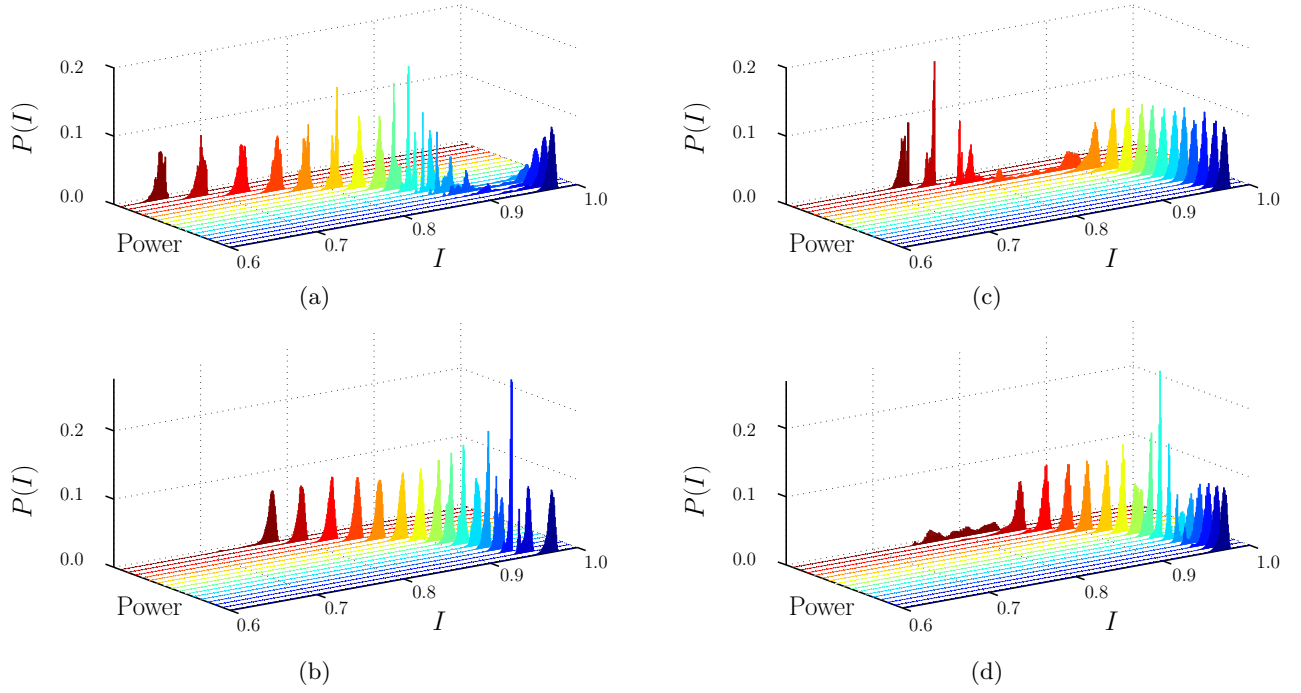


FIG. 3. (Color online) Switching current distributions for a CBJJ driven by a field. In all figures we have chosen C and R such that $\omega_0 = 0.0183 E_J/\hbar$ and $\zeta = 8.4 \times 10^{-4} E_J$. The frequencies and hence the resonance currents are chosen as $\omega_{mw} = 0.64\omega_0$, $I = 0.90$ in (a), $\omega_{mw} = 0.51\omega_0$, $I = 0.95$ in (b), $\omega_{mw} = 0.36\omega_0$, $I = 0.98$ in (c), and $\omega_{mw} = 0.255\omega_0$, $I = 0.987$ in (d). In panels (c) and (d) the resonance current is above the current of the primary zero-field peak. The applied microwave power is parametrized by the parameter, $\eta = 0, 0.002, 0.004, 0.006, 0.008, 0.010, 0.014, 0.018, 0.022, 0.030, 0.040, 0.055, 0.070, 0.090, 0.115, 0.140$, which yield the curves shown in the front (dark-blue) towards the back (dark-red) in each panel. The calculations are carried out with a bias current that increases linearly with time from $I = 0.2$ at a rate equal to $dI/dt = \frac{5E_J}{6\hbar}$. (Results are only shown for $I > 0.6$, since $P(I) \ll 1$ for the smaller bias currents.)

and renormalize with respect to the loss of norm caused by the last term.

D. Tunneling rates and switching current distributions

In a time-independent potential, the tunneling rate of the Josephson junction phase variable has been determined by Caldeira and Leggett^{24,25},

$$\gamma_{CL} = \frac{\omega_p}{2\pi} \sqrt{\frac{120\pi \cdot 7.2\Delta U}{\hbar\omega_p}} e^{-\frac{7.2\Delta U}{\hbar\omega_p} \left(1 + \frac{0.87}{\omega_p RC}\right)} \quad (9)$$

where $\Delta U = 2E_J(\sqrt{1-I^2} - I\cos(I))$ is the barrier-height, and where effects due to the friction are also taken explicitly into account.

The gradually decreasing norm, $||\psi(t)||^2$ of our numerically determined wave packet is interpreted as the probability that the phase variable has not tunneled until time t . The probability for a current switching event in the next infinitesimal time interval dt , is thus simply given by the loss of norm in that interval, and conditioned on

no previous event, the switching rate of the CBJJ reads

$$\gamma_t = -\frac{d||\psi(t)||^2}{dt} / ||\psi(t)||^2. \quad (10)$$

It is convenient in experiments to determine the switching current distribution, i.e., the probability distribution $P(I)$ for switching events to occur at different values of the bias current I , while this is being ramped up slowly, $I(t) = I_0 + \frac{dI}{dt} \cdot t$.

Our wave packet propagation yields the surviving (non-switching) population $||\psi(t)||^2$ as function of time, and we directly obtain the corresponding switching current distribution, obeying

$$\begin{aligned} P(I)\Delta I &= -\frac{d||\psi(t)||^2}{dt} \Delta t \\ &= -\frac{d||\psi(t)||^2}{dt} \left(\frac{dI}{dt}\right)^{-1} \Delta I, \end{aligned} \quad (11)$$

evaluated at the time t such that $I = I(t)$ and ΔI being the increase of I on the discrete time interval Δt .

Under the assumption of a slowly ramped bias current, the rate γ_{CL} found by Caldeira and Leggett leads to an

expression for the switching current density,

$$P(I) = \left(\frac{dI}{dt}\right)^{-1} \gamma_{CL}(I) e^{-\int_{I_0}^I \left(\frac{dI}{dt}\right)^{-1} \gamma_{CL}(I') dI'}, \quad (12)$$

which explicitly multiplies the tunneling rate with the survival probability until the value I is reached during the ramp.

In Fig. 2 we see, that our calculation indeed, reproduces the result of the quasi-static switching current distribution, (12), as function of the bias current very well in this limit.

IV. DRIVING WITH INCREASING BIAS CURRENT

We now turn on the microwave field with a constant power (constant η) and a frequency ω_{mw} , while we increase I with a low constant rate. The evolution of the system is calculated numerically using equation (8) with the potential given in (7). The parameters are chosen to represent a Josephson junction with a critical current of ~ 2 A. The results of the simulations are shown in Fig. 3(a-d), where the probability distribution is plotted. In the following subsections we will separately discuss many of the features observed in our Fig.3.

A. Resonance Peaks

The first thing we notice in Fig. 3(a) and 3(b) is that when the microwave field strength is increased, in addition to the conventional switching current peak a second peak appears. This second peak is associated with the tunnelling via the excited phase eigenstate, and hence the peak is located where the frequency $\omega_{mw} = \omega_{01}(I)$, with the resonance frequency^{26,27}

$$\omega_{01}(I) = \omega_p(I) \left(1 - \frac{5\hbar\omega_p(I)}{36\Delta U(I)}\right). \quad (13)$$

In Fig. 3(d) at a much higher field strength we observe a second peak at the same bias current as in Fig. 3(b). But, since, in this panel, the microwave frequency is half the resonance frequency, the excitation of the phase variable is a second order process²⁸.

When the power is further increased the peaks move to lower bias current, which is also well-understood²⁹. The strong microwave field then effectively suppresses the potential barrier as the power is increased.

B. Multi-peak Structure

In Fig. 3(a), after the revival of the second peak, a multi-peak structure appears. Since we only drive the junction with a single frequency field, these extra peaks cannot be understood as conventional resonances. They

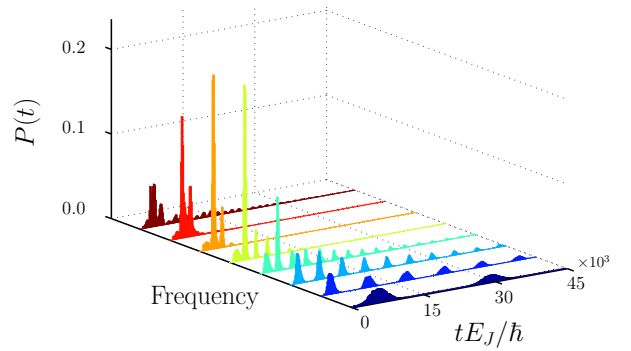


FIG. 4. (Color online) Switching current distributions for different frequency with a fixed bias current at $I = 0.96$. We have chosen C and R such that $\omega_0 = 0.0183 E_J/\hbar$ and $\zeta = 8.4 \times 10^{-4} E_J$. This gives a zero-field energy splitting between the ground and first excited states at $\omega_{01} = 0.48\omega_0$. We have increasing frequency from the closest (dark-blue) to the one farthest away (dark-red) at $\omega_{mw} = (0.036, 0.110, 0.182, 0.292, 0.365, 0.438, 0.511, 0.584)\omega_0$.

are, however, a well known effect associated with the multi-peaked Fourier transform of a frequency chirped electric field amplitude³⁰, see also³¹. The analysis in³⁰ leads to peaks with higher density for the largest detunings and, although the correspondence between the two physical problems is only approximate, it is consistent with our observation that the multi-peak structure is not discernible in Fig. 3(b). We should emphasize that in typical experiments, $\frac{dI}{dt}$ is smaller than in our calculations leading to more narrow peaks than seen here.

C. Dynamical Bifurcation

In Fig. 3(c) we see yet another interesting feature of a driven CBJJ. The resonance condition lies here at a bias current above the zero-field peak current, which implies that we see no resonance peak. However for very strong fields we observe a very broad splitting into a multi peak structure. Such results are usually explained by a dynamical bifurcation^{26,32}. Further analysis of this phenomenon is beyond the scope of the present work, but it is reassuring that our simple model also gives rise to this complex behaviour.

V. DRIVING WITH CONSTANT BIAS CURRENT

We now maintain the bias current at a constant, $I = 0.96$, close to the switching value, and we apply a microwave field to the junction. As we have already seen, the tunnelling rate is increased if the resonance condition is met. In Fig. 4 we observe what happens at different frequencies. First, the switching probability follows the field strength, but as we approach resonance,

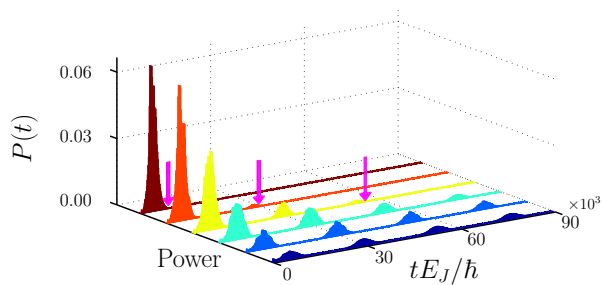


FIG. 5. (Color online) Switching current distributions for different amplitude with a fixed bias current at $I = 0.96$. We again chosen C and R such that $\omega_0 = 0.0183 E_J/\hbar$ and $\zeta = 8.4 \times 10^{-4} E_J$. This gives us $\omega_{01} = 0.48\omega_0$. We drive the junction at a very low frequency $\omega_{mw} = 0.036\omega_0$. We have increasing the power of the field from the closest (dark-blue) to the one farthest away (dark-red) at $\eta = 0.012, 0.016, 0.020, 0.024, 0.028$ and 0.032 . The arrows (mangeta) point at the spot where the summed probability for a switch is equal to unity, which in the strong field case happens after only one half cycle.

a peak emerges, and when the frequency is increased even further the peak is reduced.

A switching rate that follows the field strength in real time allows implementation of a field amplitude detector capable of resolving single oscillations of the field. In Fig. 5 we increase the field strength while maintaining a very low frequency and see that when the field is strong enough single positive oscillations of the field amplitude are clearly detected. We intend to study the performance

and sensitivity of this detection mode of the CBJJ further.

VI. CONCLUSION AND OUTLOOK

We have introduced a novel, effective method using time dependent imaginary potentials to describe the switching behaviour of a current biased Josephson junction. The method is readily implemented with standard wave packet solvers and with realistic parameters, it reproduces a wide range of results that have previously been investigated experimentally and theoretically by other techniques^{26–32}. We emphasize that our treatment builds on an ansatz for a time dependent imaginary potential (TDIP), and a number of possibilities may be explored for quantitative improvement of the potential chosen.

An advantage of the TDIP method is its ability to deal with explicitly time dependent driving fields. With the explicit treatment of the wave function of the phase variable conditioned upon the switching dynamics, we may readily extend the studies, e.g., towards modelling of the dynamics of coupled CBJJs, correlated and entangled field-CBJJ dynamics. Potentially our approach may form the basis for quantum theory of measurement, noise and back action adapted to the special field amplitude sensitivity of the device.

VII. ACKNOWLEDGEMENT

The authors acknowledge support from the EU 7th Framework Programme collaborative project iQIT.

* E-mail: ctc@phys.au.dk

¹ A. Wallraff, D. Schuster, A. Blais, L. Frunzio, R.-S. Huang, J. Majer, S. Kumar, S. Girvin, and R. Schoelkopf, *Nature* **431**, 162 (2004).

² A. Blais, J. Gambetta, A. Wallraff, D. I. Schuster, S. M. Girvin, M. H. Devoret, and R. J. Schoelkopf, *Phys. Rev. A* **75**, 032329 (2007).

³ Y. Makhlin, G. Schön, and A. Shnirman, *Rev. Mod. Phys.* **73**, 357 (2001).

⁴ G. Romero, J. J. García-Ripoll, and E. Solano, *Phys. Rev. Lett.* **102**, 173602 (2009).

⁵ B. Peropadre, G. Romero, G. Johansson, C. M. Wilson, E. Solano, and J. J. García-Ripoll, *Phys. Rev. A* **84**, 063834 (2011).

⁶ N. Grønbech-Jensen, M. G. Castellano, F. Chiarello, M. Cirillo, C. Cosmelli, L. V. Filippenko, R. Russo, and G. Torrioli, *Phys. Rev. Lett.* **93**, 107002 (2004).

⁷ J. M. Martinis, M. H. Devoret, and J. Clarke, *Phys. Rev. Lett.* **55**, 1543 (1985).

⁸ J. M. Martinis, S. Nam, J. Aumentado, and C. Urbina, *Phys. Rev. Lett.* **89**, 117901 (2002).

⁹ Y. Yu, S. Y. Han, X. Chu, S. I. Chu, and Z. Wang, *Science* **296**, 889 (2002).

¹⁰ S. Shevchenko, A. Omelyanchouk, and E. Illichev, *Low Temperature Physics* **38**, 283 (2012).

¹¹ M. Razavy, *Quantum theory of tunneling* (World Scientific, 2003).

¹² M. Devoret, A. Wallraff, and J. Martinis, arXiv preprint cond-mat/0411174 (2004).

¹³ R. De la Madrid and M. Gadella, *Am. J. Phys.* **70**, 626 (2002).

¹⁴ O. Civitarese and M. Gadella, *Physics Reports* **396**, 41 (2004).

¹⁵ A. Bohm, M. Gadella, and G. B. Mainland, *American Journal of Physics* **57**, 1103 (1989).

¹⁶ M. B. Plenio and P. L. Knight, *Rev. Mod. Phys.* **70**, 101 (1998).

¹⁷ H. M. Wiseman and G. J. Milburn, *Quantum measurement and control* (Cambridge University Press, 2010).

¹⁸ J. Dalibard, Y. Castin, and K. Mølmer, *Phys. Rev. Lett.* **68**, 580 (1992).

¹⁹ T. Sommerfeld, U. Riss, H. Meyer, L. Cederbaum, B. Engels, and H. Suter, *Journal of Physics B: Atomic, Molecular and Optical Physics* **31**, 4107 (1999).

²⁰ J. Muga, J. Palao, B. Navarro, and I. Egusquiza, *Physics Reports* **395**, 357 (2004).

²¹ G. S. Paraoanu, *Phys. Rev. B* **72**, 134528 (2005).

- ²² W. T. Strunz, Chemical Physics **268**, 237 (2001).
- ²³ J. Gambetta and H. M. Wiseman, Phys. Rev. A **66**, 052105 (2002).
- ²⁴ A. O. Caldeira and A. J. Leggett, Phys. Rev. Lett. **46**, 211 (1981).
- ²⁵ A. Caldeira and A. Leggett, Annals of Physics **149**, 374 (1983).
- ²⁶ H. F. Yu, X. B. Zhu, Z. H. Peng, W. H. Cao, D. J. Cui, Y. Tian, G. H. Chen, D. N. Zheng, X. N. Jing, L. Lu, S. P. Zhao, and S. Han, Phys. Rev. B **81**, 144518 (2010).
- ²⁷ S. Guozhu, W. Yiwen, C. Junyu, C. Jian, J. Zhengming, K. Lin, X. Weiwei, Y. Yang, H. Siyuan, and W. Peiheng, Phys. Rev. B **77**, 104531 (2008).
- ²⁸ A. Wallraff, T. Duty, A. Lukashenko, and A. V. Ustinov, Phys. Rev. Lett. **90**, 037003 (2003).
- ²⁹ M. V. Fistul, A. Wallraff, and A. V. Ustinov, Phys. Rev. B **68**, 060504 (2003).
- ³⁰ J. P. Davis and F. A. Narducci, Journal of Modern Optics **53**, 2439 (2006).
- ³¹ C. Brunel, B. Lounis, P. Tamarat, and M. Orrit, Phys. Rev. Lett. **81**, 2679 (1998).
- ³² V. E. Manucharyan, E. Boaknin, M. Metcalfe, R. Vijay, I. Siddiqi, and M. Devoret, Phys. Rev. B **76**, 014524 (2007).